THE ANNALS OF "DUNAREA DE JOS" UNIVERSITY OF GALATI
FASCICLE IX. METALLURGY AND MATERIALS SCIENCE
Nº. 3 - 2017, ISSN 1453-083X

EXAMINING THE EVOLUTION OF MICROSTRUCTURE AND ITS EFFECT ON THE MECHANICAL AND TRIBOLOGICAL PROPERTIES

Stela CONSTANTINESCU
"Dunarea de Jos" University of Galati
e-mail: constantinescu_stela@yahoo.com

ABSTRACT

This paper investigates the superior frictional performance of Ti-DLC films, by examining the evolution of microstructure and its effect on the mechanical and tribological properties. The superior frictional performance of Ti-DLC films can be attributed to the special microstructure related to the development of embedded fullerene-like microstructures as a result of incorporation of TiO_2 clusters. The factors contributing to the ultralow friction include high hardness and cohesion, excellent toughness, and high load bearing capacity (brought by the increased crosslinking and elastic energy storage ability), the friction-induced structural transformation rendering an ultralow shear resistance and the excellent resistance to oxidation-induced mechanical property degradation (due to the doped TiO_2).

The Raman, high resolution transmission electron microscopy, atomic force microscope and micro-indentation measurements consistently reveal or indicate the formation of curved graphene sheets or fullerene-like microstructures with increasing CH_4/Ar ratio.

KEYWORDS: microstructure, mechanical, tribological, frictional, wear

1. Introduction

In this work, a series of Ti-DLC films were prepared by adjusting the gas composition (i.e., CH_4/Ar ratio) and the effect of CH_4/Ar ratio on the structural, mechanical, and tribological properties of these films is examined and discussed.

Diamondlike carbon (DLC) films prepared from hydrogen-rich CH_4 source gas have been reported to exhibit a super low friction coefficient of 0.001-0.003 and wear rate of 10^{-6}-10^{-7} $mm^3/N{\cdot}m$ in dry nitrogen environment. However, such a super low friction behavior obtained from hydrogenated DLC coated surfaces cannot be sustained under ambient conditions due to the potential destruction by oxygen when exposed to air [1].

Various methods have been taken to address this issue and one commonly employed method is to incorporate metal or nonmetal elements into the carbon matrix [2-5]. But the choice of dopant plays a significant role in tailoring specific properties of DLC films for desired applications [6]. Of those doped elements, titanium has been selected because of its good adhesion to most substrate materials and easy reaction with carbon [7]. The TiC-rich surface is able to greatly improve the oxidation resistance of DLC films by forming a diffusion barrier to hinder the diffusion of into the sublayer, which is much helpful to prevent the incursion and destruction of to the cross-linked carbon network.

Extensive studies on the microstructural, mechanical, and tribological properties of Ti-doped carbon films have been reported [8-10]. Tribologically, the investigation of Ti-DLC films has been carried out in a wide range of normal load, ranging from micro-Newton and milli-Newton, aiming at possible application to micro electromechanical systems and micromechanical assemblies, to about 100 N, in order to meet the needs of the service requirement of high precision ball bearing and automotive parts that are often subjected to high applied load.

Usually, a higher TiC concentration (e.g., >25 %) in TiC/a-C:H films would give friction coefficients 0.1-0.3 when sliding against steel balls at room temperature [11, 12].

However, it was reported an ultralow friction of <0.025 in dry air for TiC/a-C:H films with a TiC fraction higher than 25%. A glassy microstructure with fine TiC microparticles (e.g., 2 μm) embedded in

hydrocarbon matrix was reported to show excellent toughness and wear resistance due to suppressed microcrack propagation [13, 14]. To the best of our knowledge, however, few studies have been reported on Ti-DLC films showing an ultralow friction performance (COF < 0.015). Based on previous work in synthesizing ultralow friction pure carbon films, we synthesized a new kind of Ti-doped DLC films [15].

The Ti-DLC films showed an ultralow and steady friction behavior (0.008-0.015) in ambient air and nearly independent of counterpart materials. A combined effect of the inherent mechanical properties, the friction-induced structural transformation, and the presence of a transfer film was proposed to explain the lubrication performance. However, it remains unclear to what degree the microstructure and/or the mechanical properties will affect the friction and wear of Ti-DLC films and how they affect it. More efforts are needed to clarify the mechanism and, if possible, to intentionally design the structure to make the ultralow and steady friction behavior controllable.

2. Experiment

2.1. Film deposition and characterization

Ti-DLC films were deposited on polished substrates and n-type Si (100) wafers by a hybrid radio frequency enhanced chemical vapor deposition (CVD) [15]. A mixture of CH_4 (99.99%) and Ar (99.99%) was used as the source gas of CVD to synthesize carbon film into which titanium was doped the titanium (99.99%) targets. The mass flow rate ratio of CH_4 to Ar (CH_4/Ar) was adjusted from 27% to 50% in gas mixture under a constant working pressure. Detailed deposition parameters are listed in Table 1. An adhesive interlayer of Si, 5-10 µm thick, was deposited silicon targets (99.999%). The overall film thickness was 10 ± 0.1 µm. A non-doped DLC film was also prepared for comparison.

Table 1. *Deposition parameters for Ti-DLC films*

Parameter	Value			
Working pressure (Pa)	0.6			
Ti target current (A)	4.0			
Bias frequency (kHz)	30			
Duration (min)	120			
Mass flow rate of CH_4 (sccm)	34	45	54	60
Mass flow rate of Ar (sccm)	68	60	54	48
CH_4/Ar ratio	27% (Film 1)	35% (Film 2)	43% (Film 3)	50% (Film 4)

The microhardness and elastic modulus of the films were determined using a Micro-Hardness Tester (MTS Indenter XP). Five indentations were made for each sample, and the hardness was calculated by averaging five measurements from loading–unloading curve. The elastic recovery was calculated using the formula (dmax_dmin)/dmax, where dmax and dmin are the maximum and minimum displacement during unloading, respectively.

Frictional properties of the Ti-DLC films were evaluated on a reciprocating-type ball-on-flat tribometer (CSM), which was equipped with a chamber where the relative humidity and gaseous environment could be controlled. Sliding tests were performed in ambient air environment at an average sliding velocity of 90 mm/s under room temperature.

Si_3N_4 ball (~ 6 mm in diameter) was used as the counter face. Worn surfaces of films and mated balls were observed on an Olympus STM6 Measuring Microscope and a MicroXAM surface mapping microscope.

High resolution transmission electron microscopy (HRTEM) images were obtained on a JEOL 2010 TEM operated at 200 kV. The film sample for HRTEM observation was first deposited on NaCl substrates followed by dissolution of the

NaCl substrate with deionized water was used. The surface morphology of the films was observed using a Digital Instruments Nanoscope III Multimode atomic force microscope (AFM). The cross-section micrographs were obtained on a field emission scanning electron microscope (FESEM, JEOL JSM-6701F).

3. Results and discussion

Fig. 1, the microhardness, elastic modulus, and elastic recovery of films consistently increase with increasing CH_4/Ar ratio. The hardness grows monotonically from 8 MPa at CH_4/Ar¼27 % to 14 MPa at 50 %. Correspondingly, the elastic recovery increases from ~65 % to ~70 %.

To better understand the microstructural evolution as a function of CH_4/Ar ratio and its correlation to the Raman spectra, the Ti-DLC films were characterized by HRTEM and FESEM.

Figure 2 shows the HRTEM plan-view images of four Ti-DLC films. As shown, planar graphene sheets greater than 5 μm could be seen at 27 %. However, once the CH_4/Ar ratio was raised to 35 %, a considerable amount of short-length curved sheets starts to show up. A further development of curved sheets into closed-cage fullerene-like structures could be seen at CH_4/Ar¼43 %.

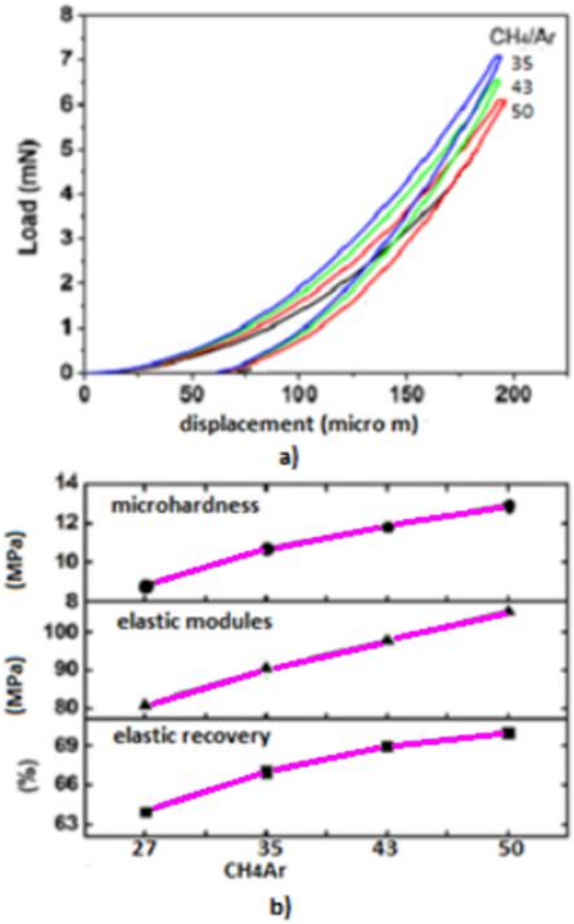

Fig. 1. *(a) Micro-indentation load–displacement curves for Ti-DLC films. (b) Calculated hardness, elastic modulus, and elastic recovery*

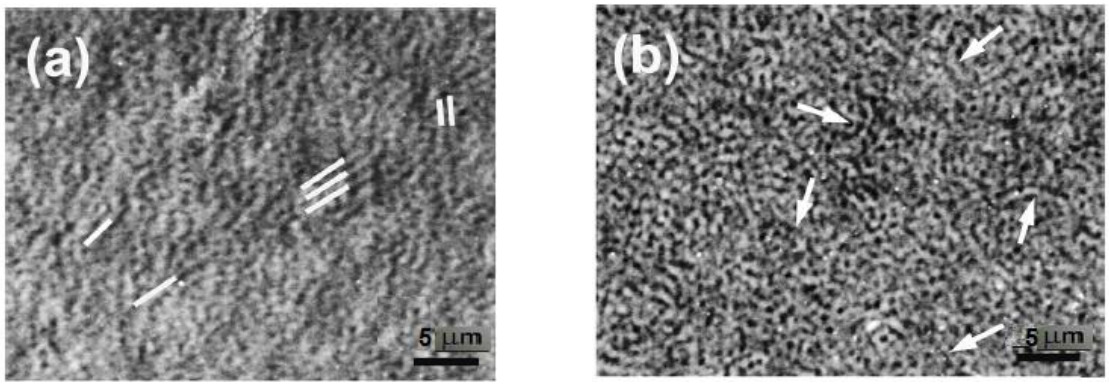

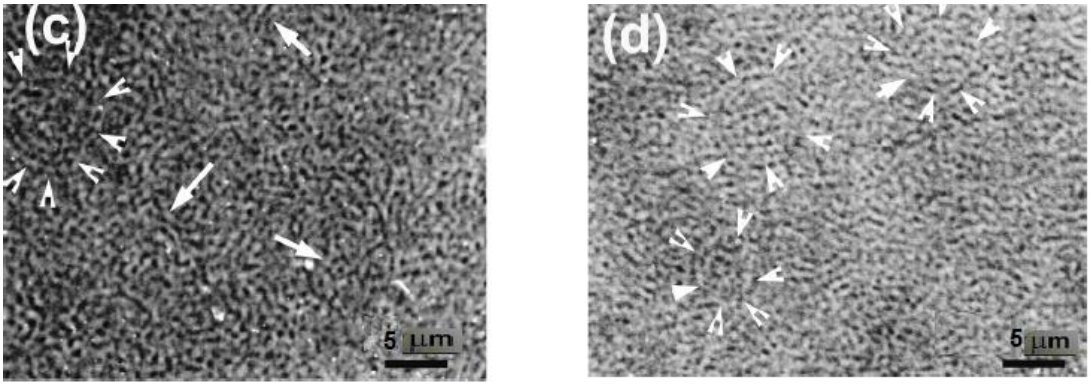

Fig. 2. *HRTEM plan-view images for the films. The arrows show the curved sheets or closed cage structure*

Then, with a further increase in CH_4 to 50 %, a greater amount of multi-shell fullerenes (carbon inions) tend to form. Since the hardness has been proposed to correspond to the density of enthalpy of many hard-homogeneous bulk materials, that is, the number of bonds per unit volume multiplying the binding energy of each bond, or, in other words, the cohesion energy of the material, the enhanced elastic recovery should be due to the increased amount of resilient structures such as curved graphene sheets, close-caged fullerene, and multi-shell carbon inions. The cross-sectional FESEM micrographs of two typical films (27 % and 50 %) are shown in Fig. 3.

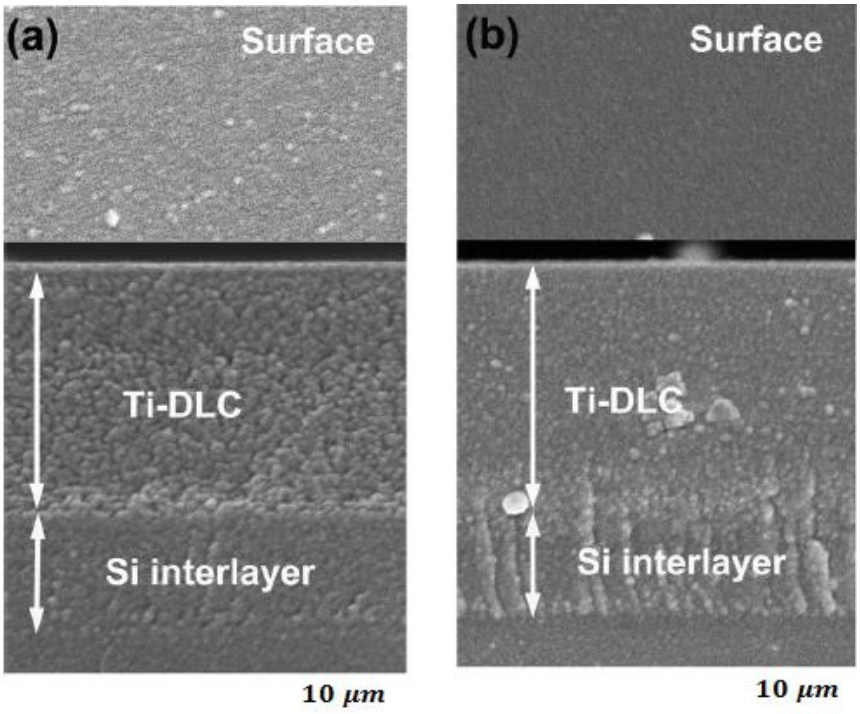

Fig. 3. *Cross-sectional and surface FESEM micrographs of two typical films: (a) CH_4/Ar ¼ 27 % and (b) CH_4/Ar ¼ 50 %*

The surface images are also given for comparison. As seen, larger-size particles are generated at 27 %, thus leading to a more porous structure and rougher surface. By comparison, the fine particles at 50 % give a denser structure without clearly visible pores and the surface is much smoother. To further examine the surface topography of Ti-DLC films, AFM characterization was conducted and the images are shown in Fig. 4. A smoothened surface could be clearly seen with increasing CH_4/Ar ratio. The average energy per carbon atom would be higher at CH_4/Ar¼27 % than

at CH_4/Ar¼50 %. This would lead to a larger thermal spike volume and higher mobility and thus promote the formation of more graphitic clusters at CH_4/Ar¼27 %. In addition, the higher energy of carbon species may increase the possibility of C-Ti bonding and also the surface growth of graphitic carbon film, as described in the sub plantation model. The combined effect of surface growth and TiC microparticles may account for the higher surface roughness at CH_4/Ar¼27 %. As the CH_4/Ar increases to 35 %, the average energy per carbon atom drops to a lower level, which would increase the fraction of sub-planted carbon atoms due to reduced mobility. The formation of fullerene-like structures in carbon films is conditional, depending on the ion impact energy, substrate temperature, duty cycle of bias, and incorporation of proper foreign atoms like nitrogen and their concentration.

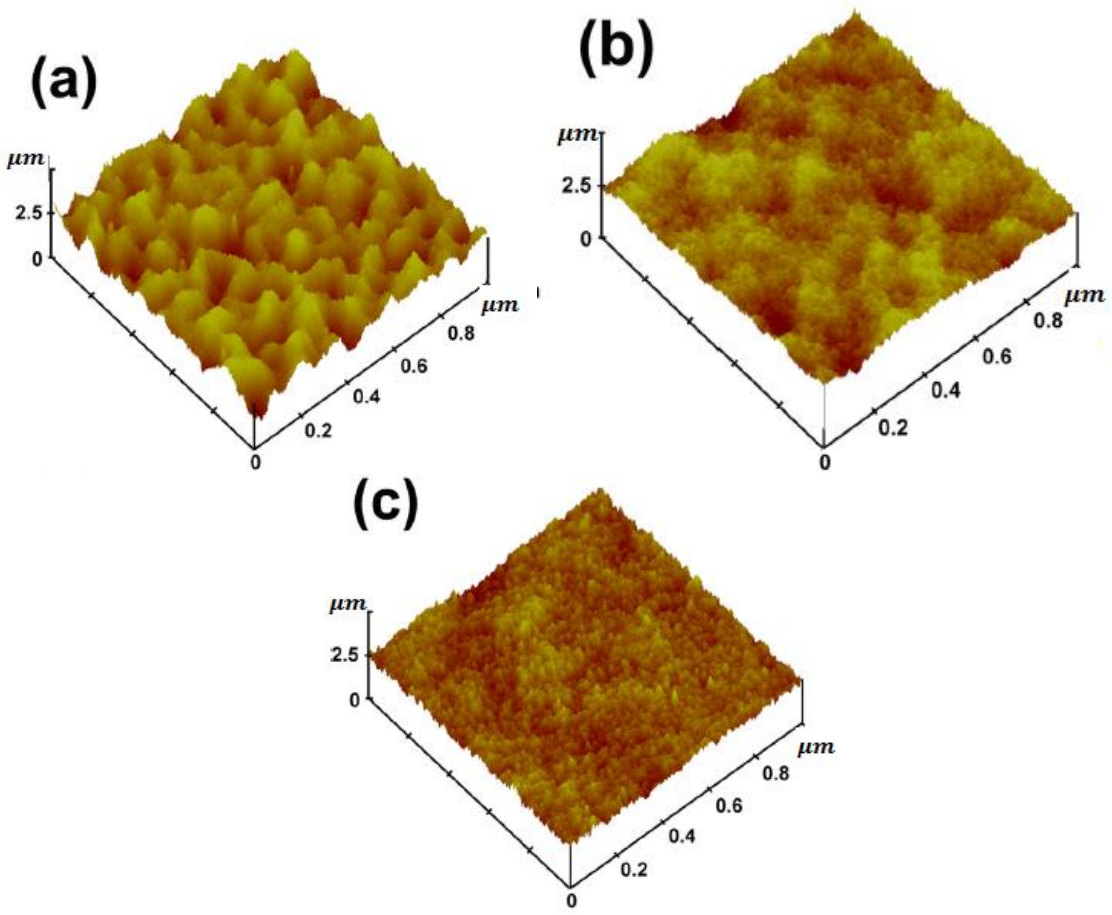

Fig. 4. *AFM images of Ti-DLC films prepared at different CH_4/Ar ratios: (a) 35 %, (b) 43 %, and (c) 50 %*

For present Ti-DLCs, the evolution of curved graphene sheets or fullerene-like onions is considered to be due to the catalysis effect of doped TiO_2 because major curved structures were observed at the edge of TiO_2 clusters, which will be discussed in detail elsewhere. In addition, the effect of proper ion incident energy per carbon atom and the size of embedded TiO_2 clusters size should also be taken in to account because a more graphitic microstructure has been found even at a higher concentration of TiO_2.

The evolution of microstructure as a function of CH_4/Ar ratio leads to totally different mechanical and tribological properties of Ti-DLC films. Apart from the difference in hardness and elastic recovery, the cohesion and toughness of films also differ from each other. As shown in Fig. 5, when the films delaminate from stainless Steel surface without Si interlayer as a result of accumulated internal stress, the film 1 at 27 % tends to break into small pieces, indicating the brittle nature of it. For film 2, however, it would wrinkle to release stress, with only minor cracks. Further improvement of toughness could be seen for

film 3 and film 4, which do not show any visible cracks.

Figure 3 shows the optical micrographs of Ti-DLC films peeled off from interlayer free substrates as a result of internal stress.

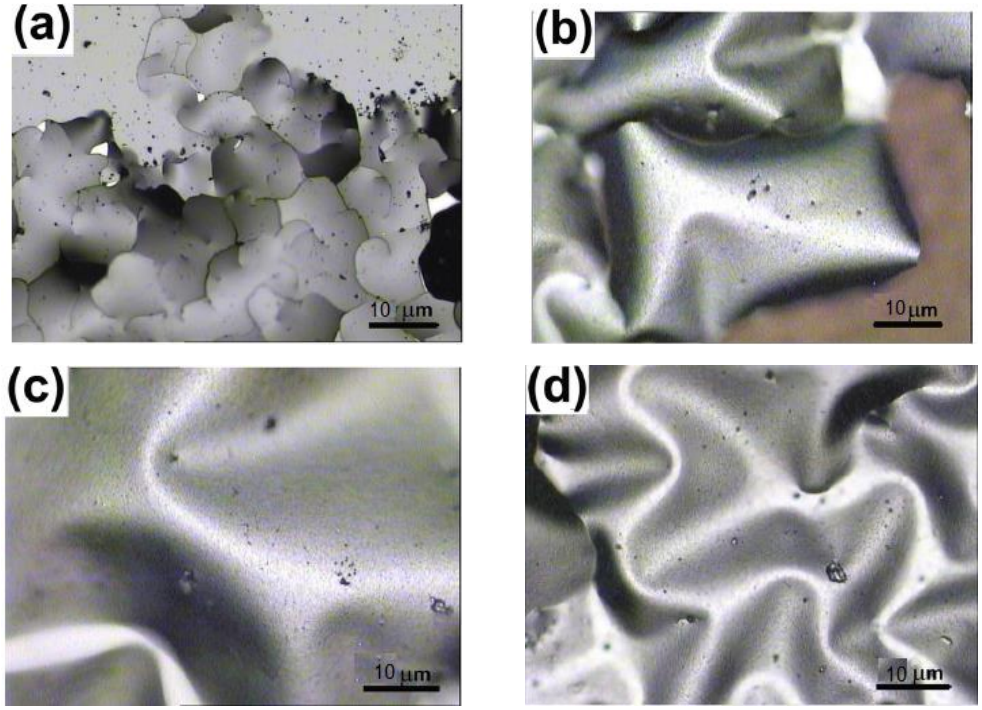

Fig. 5. *Optical micrographs of Ti-DLC films peeled off from interlayer substrates as a result of internal stress*

Figure 6 shows the friction behavior of Ti-DLC films sliding against Si_3N_4 balls under a normal load of 10 N in ambient air environment. The corresponding wear rate of each film is given in Fig. 7. Generally, the increased CH_4/Ar ratio leads to gradually reduced friction coefficient and wear rate. As seen, the friction behavior of film-1 is much different from that of the other three films, which could be expected from the above characterizations of microstructure and mechanical properties.

For film 1, the friction coefficient is unstable and increases rapidly with sliding distance, reaching ~0.10 at the end of the test. The corresponding wear rate is ~$2.8x10^{-6}$ $mm^3/N{\cdot}m$. While the other three films all show very smooth friction curves, and the steady state friction coefficient drops from ~0.012 for film 2 to ~0.008 for film 4. Correspondingly, the specific wear rate decreases from ~$3.1x10^{-7}$ $mm^3/N{\cdot}m$ for film 2 to ~$1.2x10^{-7}$ $mm^3/N{\cdot}m$ for film 4, 1 order of magnitude lower than that of film 1.

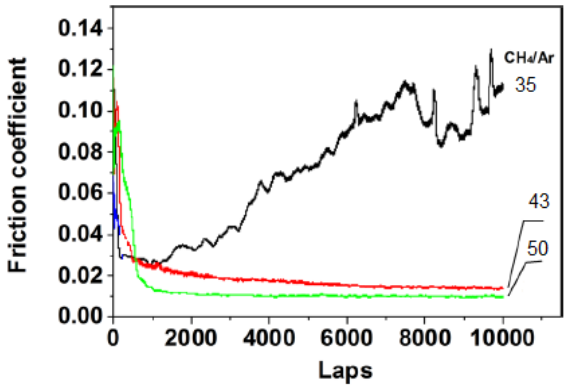

Fig. 6. *Friction curves of Ti-DLC films sliding against Si_3N_4 balls (d ¼ 6 mm) in ambient air. Normal load: 10 N; mean velocity: 90 mm/s*

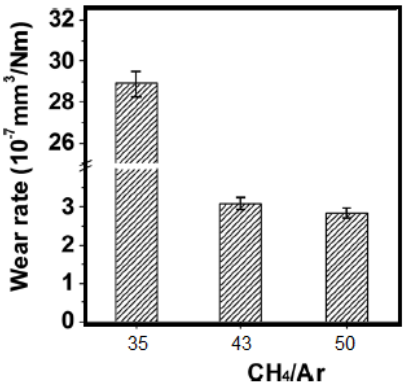

Fig. 7. *Specific wear rate of Ti-DLC films*

Figure 8 shows the optical micrographs of wear tracks of films and wear scars on mating balls after friction tests. The 3D micrographs of wear tracks and the corresponding cross-sectional profiles are given in Fig. 9. As seen, the wear track of film 1 [Fig. 8(a)] is clearly different from the others [Figs. 8(b)–8(c)]. A large number of black debris can be seen both inside and outside the wear track. And the wear track shows a width of ~5 μm and a depth of ~3 μm. The wear depth is much higher than the film thickness, indicating that the film has been worn out by the end of the test (due to the low hardness and brittleness). Hence, for film 1, the friction test was actually conducted between Si_3N_4 ball and steel substrate rather than the Ti-DLC film. As a result, it does not only make the friction coefficient increase with great fluctuation, but also leads to severe wear of the mated ball which shows deep scratches on the worn surface [Figs. 8(b1) - 8(c1)]. In contrast, the wear for film 2 to film 3 is much milder. The width of all the three wear tracks is below 2 μm, and the depth only 8-10 μm (the wear scar becomes gradually shallower with increased CH_4/Ar ratio). For the mated balls, no scratched grooves due to abrasive wear could be seen, with only a layer of transferred film on the worn surface.

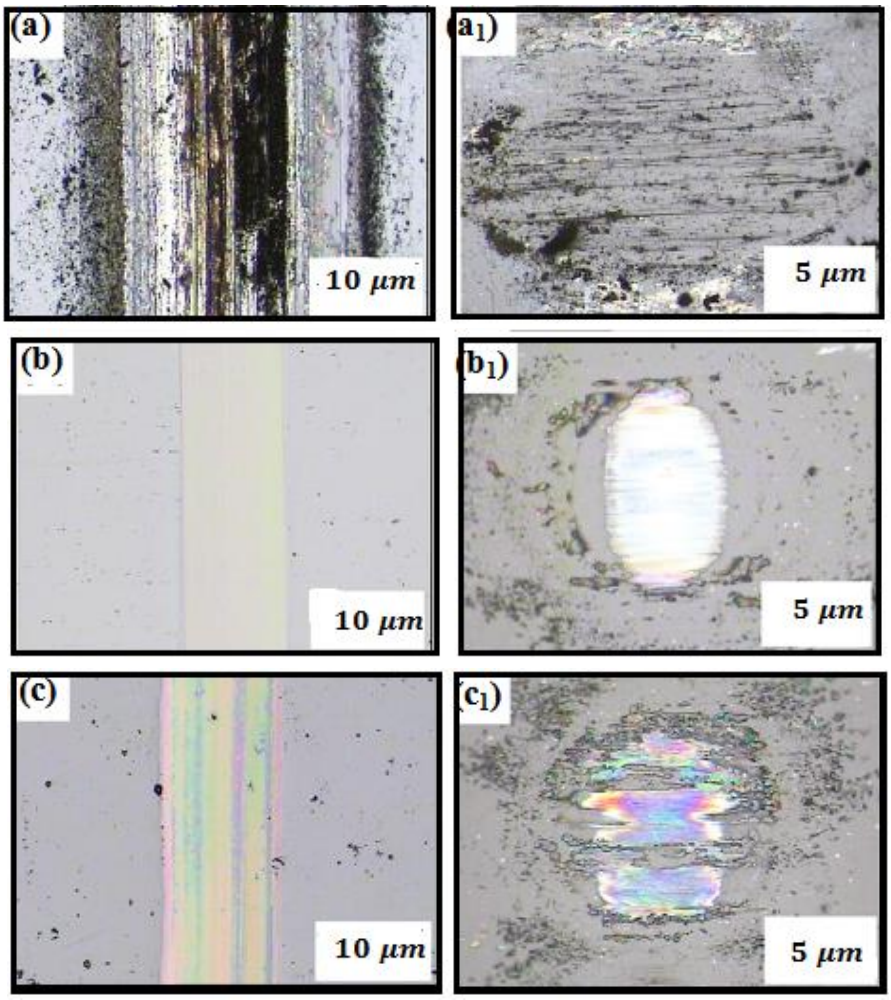

Fig. 8. *Optical micrographs of wear tracks on films and wear scars on balls after friction tests. (a) and (a1): CH_4/Ar ¼ 35 %; (b), (b1): CH_4/Ar¼ 43 %; (c) and (c1): CH_4/Ar ¼ 50 %*

The friction and wear result once again confirm the better toughness and cohesion strength of films 2, 3, and then film 1, which leads to less possibility of brittle fracture and abrasive wear induced by hard particles. Therefore, the friction coefficient remains stable in the whole course of test. Moreover, the wear of films in this case should be dominated by adhesion, which transfers film to the mated ball surface during repeated rubbing process. The wear mode transition from abrasive wear to adhesive wear with reduced amount of incorporated metal is consistent with the previous study [16]. Usually, a higher cohesion strength and hardness would lead to less severity of adhesion wear. Moreover, the wear rate drops from film 2 to film 3 with gradually shallower wear track. It keeps decreasing from film 2 to film 3, Fig. 6, even with a deteriorated continuity of the transfer film [Fig. 8(b1)]. The ultralow and steady friction behavior of Ti-DLC films has been discussed previously by the authors from the perspectives of inherent film property, the friction induced structural transformation, and the transferred layer on mated ball 42.

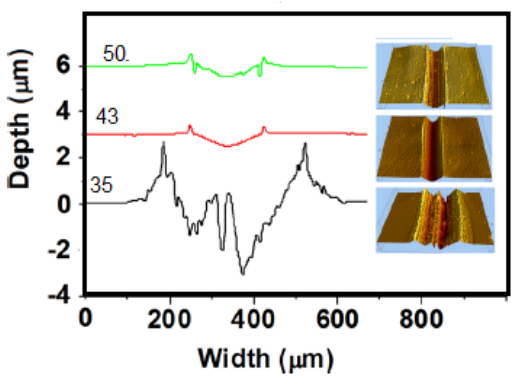

Fig. 9. *D micrographs of wear tracks and the corresponding cross-sectional profiles*

This paper further investigates the superior frictional performance of Ti-DLC films, by examining the evolution of microstructure and its effect on the mechanical and tribological properties. The superior frictional performance of Ti-DLC films can be attributed to the special microstructure related to the development of embedded fullerene-like microstructures as a result of incorporation of TiO_2 clusters and proper ion impact. This special structure with increased crosslinking and elastic energy storage ability leads to enhanced hardness and cohesion, improved toughness, and load-bearing capacity (resilient to withstand severe deformation) together with the surface structure transformation to render ultralow interfacial resistance and the excellent resistance.

4. Conclusions

An ultralow and steady friction behavior (0.008-0.01) in ambient air was shown by previously prepared Ti-doped DLC films. The initial examination revealed a combined effect of several factors that might contribute to the ultralow friction behavior, including inherent mechanical properties, the friction-induced structural transformation, and the presence of a polymerlike thin transfer film. To clarify the effect of microstructure and composition on the mechanical and tribological properties of the low friction Ti-DLC films, and thus to make the ultralow friction behavior controllable by intentional structural design, we synthesized a series of Ti-DLC films with varied microstructure and Ti content by adjusting feed gas composition (i.e., CH_4/Ar ratio). The characterization results reveal that the low CH_4/Ar ratio of 27 % would lead to a higher Ti-doping content (~6.5 at.%) and promote the formation of Ti-C clusters. However, the higher average energy per carbon atom in this case would also lead to the formation of graphitic clusters (planar sheets in HRTEM images) both inside the carbon matrix and on the growing surface, thus resulting in a rough surface and low hardness even in the presence of a considerable amount of TiC clusters. The increased CH_4/Ar ratio to 35 % would reduce the impact energy of incident carbon atoms and increase the fraction of sub planted carbon atoms due to reduced mobility

The increased local stress could force curvature in graphitic clusters and result in the evolution of odd-membered carbon rings. The increased cross-linking drastically improves the mechanical properties of Ti-DLC films, including greatly enhanced toughness, elastic recovery, and hardness. Further increase in CH_4/Ar ratio to 43 % promotes the formation of more curved graphene sheets and some close caged structures start to show up. As the CH_4/Ar ratio was raised to 50 %, multi shell carbon onion structures embedded in the carbon matrix could be seen and higher hardness, higher cohesion, higher elastic recovery, and lowest friction coefficient (<0.01) were shown. The formation of fullerene-like microstructures in present Ti- DLC films seem to be through the latter path, because major curved structures were observed at the edge of TiO_2 clusters. Further efforts to analyze the catalysis effect of doped TiO_2 are needed.

To sum up, this paper investigates the superior frictional performance of Ti-DLC films, by examining the evolution of microstructure and its effect on the mechanical and tribological properties. The superior frictional performance of Ti- DLC films can be attributed to the special microstructure related to the development of embedded fullerene-like microstructures as a result of incorporation of TiO_2

clusters. The factors contributing to the ultralow friction include high hardness and cohesion, excellent toughness, and high loadbearing capacity (brought by the increased crosslinking and elastic energy storage ability), the friction-induced structural transformation rendering an ultralow shear resistance and the excellent resistance to oxidation-induced mechanical property degradation (due to the doped TiO_2).

References

[1]. Erdemir O. L. Eryilmaz, Fenske G., J. Vac. Sci. Technol., A 18, 1987, 2000.
[2]. Galvan Y. T. Pei, De Hosson J. T. M., Surf. Coat. Technol. 201, 590, 2006.
[3]. Dimigen, Kiages C.-P., Surf. Coat. Technol., 49, 543, 1991.
[4]. Gilmore, Hauert R., Thin Solid Films, 398-399, 199, 2001.
[5]. Erdemir, Donnet C., J. Phys. D., Appl. Phys., 39, 311, 2006.
[6]. Gayathri, Kumar N., Krishnan R., Ravindran T. R., Amirthapandian S., Dash S., Tyagi A. K., Sridharan M., Ceram. Int. 41, 1797, 2015.
[7]. Kulikovsky Y., Fendrych F., Jastrabik L., Chvostova D., Surf. Coat., Technol., 91, 122, 1997.
[8]. Bharathy V., Nataraj D., Chu P. K., Wang H., Yang Q., Kiran M. S. R. N., Silvestre-Albero J., Mangalaraj D., Appl. Surf. Sci. 257, 143, 2010.
[9]. Pauleau, Thie`ry F., Surf. Coat. Technol., 180-181, 313, 2004.
[10]. Tsai C., Hwang Y.-F., Chiang J.-Y., Chen W.-J., Surf. Coat. Technol., 202, 5350, 2008.
[11]. Zehnder, Patscheider J. O., Surf. Coat. Technol., 133-134, 138, 2000.
[12]. Zhang X. L. Bui, Jiang J., Li X., Surf. Coat. Technol., 198, 206, 2005.
[13]. Pei T., Huizenga P., Galvan D., Hosson J. T. M. D., J. Appl. Phys., 100, 114309, 2006.
[14]. Pei T., Galvan D., De Hosson J. T. M., Acta Mater., 53, 4505, 2005.
[15]. Zhao H. Li, Ji L., Wang Y., Zhou H., Chen J., Diamond Relat. Mater., 19, 342, 2010.
[16]. Han F. Yan, Zhang A., Yan P., Wang B., Liu W., Mu Z., Mater. Sci. Eng., A 348, 319, 2003.